Three-body Effects in Calcium(II)-ammonia Solutions: Molecular Dynamics Simulations

Wiwat Sidhisoradej, Supot Hannongbua^a, and David Ruffolo

Department of Physics (^a Department of Chemistry), Faculty of Science, Chulalongkorn University, Bangkok 10330, Thailand

Z. Naturforsch. 53a, 208-216 (1998); received February 16, 1998

Molecular dynamics simulations have been performed with and without three-body corrections at an average temperature of 240 K using a flexible ammonia model. The system consists of one calcium ion and 215 ammonia molecules. The calcium(II)-ammonia interactions were newly developed, based on *ab initio* calculations with a basis set of double zeta quality. The role of three-body interactions on the structural and dynamical properties of the solution has been investigated. The presence of three-body corrections leads to the reduction of the first shell coordination number of Ca(II) in liquid ammonia from 9 to 8, the increase of the size of the solvation shell by 0.33 Å and the disappearance of the second solvation shell.

1. Introduction

It has been known since the early 1940s that manybody effects can have an important influence on the results obtained from computer simulations. This can lead to a serious modification of the simulation models, especially in cases of condensed-phase systems [1]. In 1962, in order to simplify the calculation of many-body exchange effects, Jansen [2] introduced the Gaussian effective electron model and found that first-order three-body exchange effects for the rare gases could change the exchange energies by as much as 20% of the two-body exchange energies. Furthermore, Lombardi and Jansen [3] also extended the approach to four-body interactions and found that these effects were negligible for most geometries of interest. These observations have been illustrated for a monatomic gas [4] and numerous cases of ions in aqueous solution [5-8]. In addition, recent studies of Na(I), Mg(II), or Zn(II) solvation in liquid ammonia by Monte Carlo simulations showed that the three-body corrections reduce their first shell coordination number from 9 to 8, 10 to 6, or 9 to 6, respectively [9-10]. Ab initio calculations with double zeta quality basis sets for the corresponding octahedral ion-ammonia complexes showed that the error in the two-body approximation of the binding energy was 17%, 30%, or 18%, respectively. However, similar investigations for Li(I) in liquid ammonia [11] showed that adding three-body corrections did not influence the first shell coordination number of 6, even though the pair approximation overestimated the octahedral Li(NH₃)₆ complex binding energy by 23%.

In the present work, the role of three-body effects on the structural and dynamical properties of a Ca(II)-ammonia solution has been analyzed using the molecular dynamics method. Two simulations have been performed, with and without three-body correction functions, using newly developed Ca(II)-NH₃ pair potential and NH₃-Ca(II)-NH₃ three-body correction functions.

2. Details of the Calculations

2.1 Development of the Ca(II)-NH₃ Pair Potential

To cover a range of NH₃ distances and orientations relative to Ca(II), more than 1700 Ca(II)-NH₃ pair configurations were generated. The experimental gas phase geometry of the ammonia molecule, with an N-H distance of 1.0124 Å and HNH angle of 106.67°, was taken from the literature [12] and kept constant throughout. The pair interaction energies were computed using *ab initio* self-consistent fiend (SCF) calculations with double zeta quality basis sets including polarization functions, and were fitted to an analytical function of the form

$$\Delta E_{2b \text{ fit}} = \sum_{i=1}^{4} \left[\frac{a_i}{r_i^4} + \frac{b_i}{r_i^3} + c_i \exp(-d_i r_i) + \frac{332.15 q_i q_{\text{Ca}}}{r_i} \right], (1)$$

where $\Delta E_{2b \, \text{fit}}$ is the fitted energy in kcal·mol⁻¹, a_i , b_i , c_i , and d_i are the fitting parameters, r_i is the distance in Å

Reprint requests to Dr. S. Hannongbua, Fax: (662) 2521730.

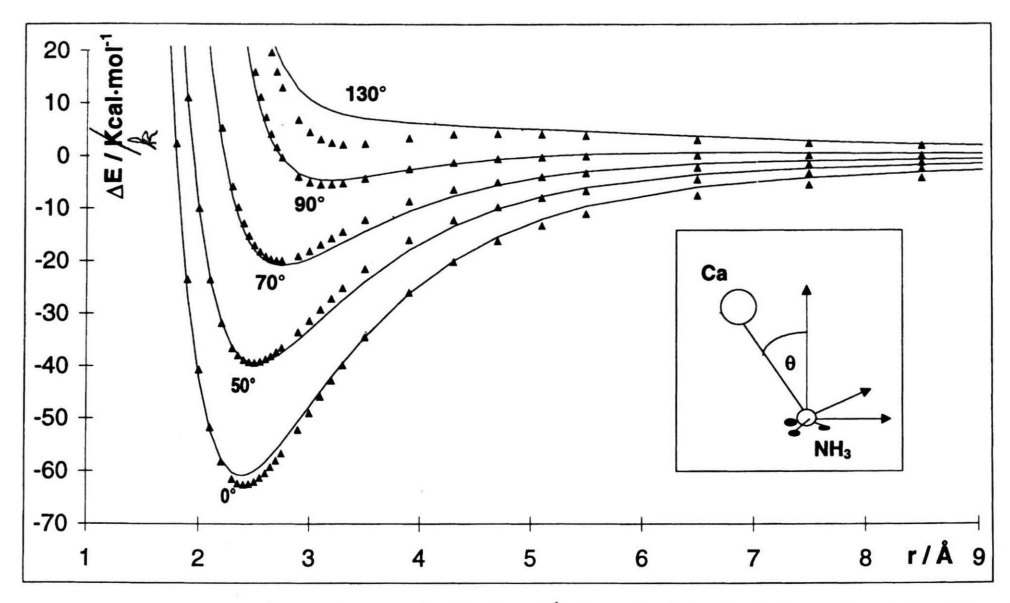


Fig. 1. Ca(II)-NH₃ dimer interaction energies (kcal·mol⁻¹) from *ab initio* calculations (triangles) and from best-fit pair potential functions (solid lines).

Table 1. Optimized parameters a, b, c, and d of the analytical pair potential function along with q values (in atomic units) derived from the ab initio calculations (see text for details).

	$a \text{ (kcal} \cdot \text{Å}^4 \cdot \text{mol}^{-1})$	$b \pmod{(kcal \cdot \mathring{A}^3 \cdot mol^{-1})}$	$_{(\text{kcal} \cdot \text{mol}^{-l})}^{c}$	d (Å ⁻¹)	q	
Ca-N	3614.1584	-768.5588	-1083.0971	0.9954	-0.8340	
Ca-H	405.7155	173.4295	-3051.4211	2.3356	0.2780	

between the *i*-th atom of the ammonia molecule and the calcium ion, and q_i and q_{Ca} are their corresponding atomic net charges obtained from a Mulliken population analysis [13] in the SCF calculations. The final values of the fitting parameters for the Ca(II)-NH₃ pair potential, using a non-linear least squares fitting method, are given in Table 1. The SCF and the fitted energies for some trajectories, including the most favourable configuration where the dipole moment of the ammonia molecule points away from the ion, are compared in Figure 1.

2.2 Development of the NH₃-Ca(II)-NH₃ Three-body Correction Function

As illustrated in Figure 2, for three-body calculations, the nitrogen atom of the first ammonia molecule, N1, was at the origin of the coordinate system, and the calcium ion was along the z-axis at a distance r_1 from N1. The ni-

trogen atom of the second ammonia molecule, N2, was placed at the coordinates (r_2, θ_2, ϕ_2) . Both ammonia molecules are in the configuration in which their dipole vectors point to the calcium ion. The four parameters were varied independently in the ranges $1.9 \text{ Å} \leq r_i \leq 10.0 \text{ Å}$, $0^\circ \leq \theta_2 \leq 180^\circ$, and $0^\circ \leq \phi_2 \leq 60^\circ$ in order to cover the whole spatial configuration of the NH₃-Ca(II)-NH₃ complex. Then the three-body interaction energy, ΔE_{3b} , for each configuration was computed from the SCF energies of the monomer, dimer, and trimer according to the equation:

$$\Delta E_{3b} = [E\{ML_1L_2\} - E\{M\} - E\{L_1\} - E\{L_2\}]$$

$$-[E\{ML_1\} - E\{M\} - E\{L_1\}]$$

$$-[E\{ML_2\} - E\{M\} - E\{L_2\}]$$

$$-[E\{L_1L_2\} - E\{L_1\} - E\{L_2\}],$$
(2)

where M, L_1 , and L_2 denote the calcium ion and the first and second ammonia molecules, respectively. The three-body interaction energy was fitted using an analytical function of the form

$$\Delta E_{3h \text{ fit}} = \{ R_1(r_1) R_2(r_2) + R_1(r_2) R_2(r_1) \} \Theta(\theta), (3)$$

where

$$R_1(r_1) = (a_0^{(1)} + a_1^{(1)}r_1 + a_2^{(1)}r_1^2 + a_3^{(1)}r_1^3) \exp(-c_1^{(1)}r_1),$$

$$R_2(r_2) = (a_0^{(2)} + a_1^{(2)}r_2 + a_2^{(2)}r_2^2 + a_3^{(2)}r_2^3) \exp(-c_1^{(2)}r_2),$$

$$\Theta(\theta) = (a_0^{(3)} + a_1^{(3)}\cos\theta + a_2^{(3)}\cos^2\theta + a_3^{(3)}\cos^2\theta)$$

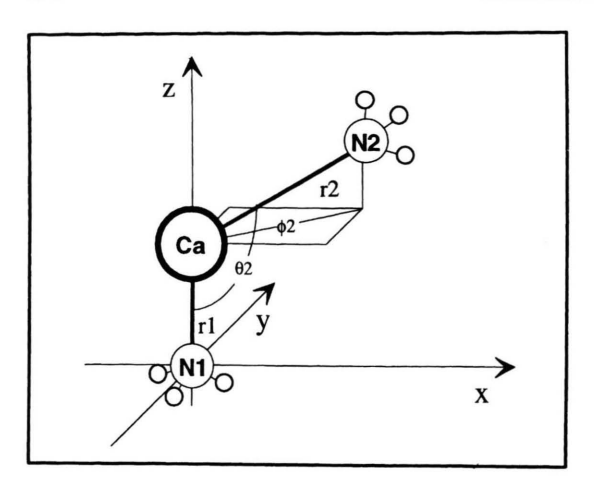


Fig. 2. Geometry for the evaluation of the $\mathrm{NH_3\text{-}Ca(II)\text{-}NH_3}$ potential for SCF calculations and the three-body correction function.

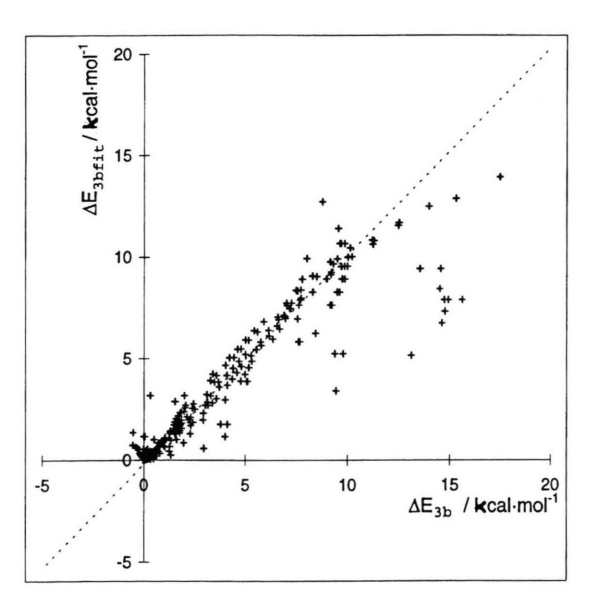


Fig. 3. Comparison of ΔE_{3b} (SCF) and $\Delta E_{3b\, {\rm fit}}$ for a random sample of the generated configurations.

were employed, where $a_j^{(i)}$ and $c_j^{(i)}$ are fitting constants and θ is the N₁-Ca(II)-N₂ angle. The optimal values of the parameters are given in Table 2 while the SCF and fitted energies are compared in Figure 3. Three-dimensional plots of $\Delta E_{3b\, {\rm fit}}$, r_2 and θ in the configuration shown in Fig. 2 at r_1 =1.5 Å, 2.0 Å, 2.5 Å and 3.0 Å are displayed in Figure 4.

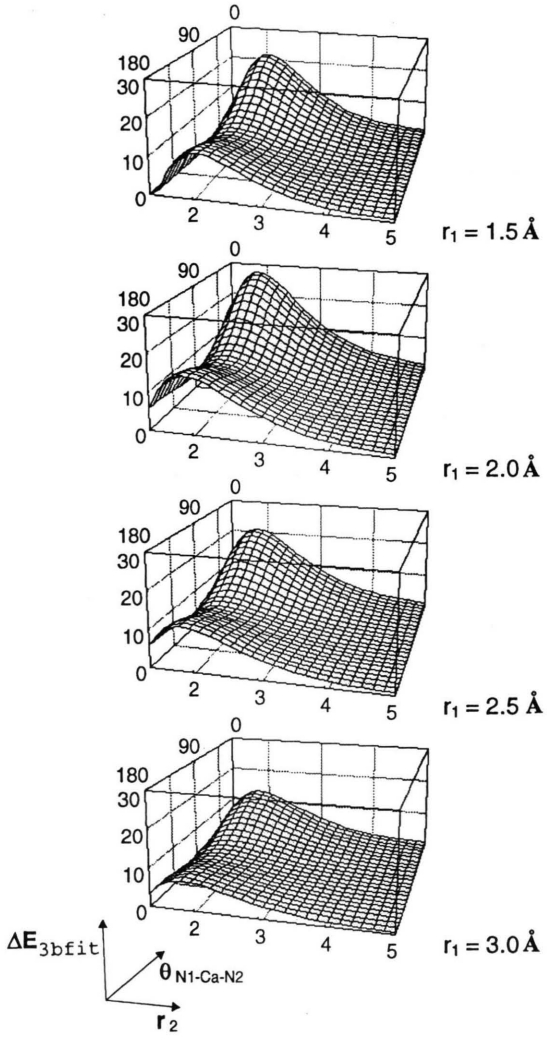


Fig. 4. Potential energy surface for the three body effect $(\Delta E_{3b \, \text{fit}} \text{ in kcal} \cdot \text{mol}^{-1})$ in the NH₃-Ca(II)-NH₃ complex as a function of the N2-Ca(II) distance $(r_2 \text{ in } \text{Å})$ and N1-Ca(II)-N2 angle $(\theta \text{ in degrees})$ at constant N1-Ca(II) distance, r_1 =1.5, 2.0, 2.5, and 3.0 Å (see Figure 2).

Table 2. Optimized parameters $a_j^{(i)}$ and $c_j^{(i)}$ of the analytical 3-body correction functions $(r \text{ in } \text{ Å} \text{ and interaction energies in kcal} \cdot \text{mol}^{-1})$.

	i=1	<i>i</i> =1	i=1	
$a_0^{(i)}$	-26.1335	26.7764	1.8751	
$a_1^{(i)}$	-0.0166	-29.0045	-0.8993	
$a_2^{(i)}$	0.4367	8.4738	1.8335	
$a_3^{(i)}$	0.0303	-0.7836	-0.1777	
$a_0^{(i)}$ $a_1^{(i)}$ $a_2^{(i)}$ $a_3^{(i)}$ $c_1^{(i)}$	0.7031	1.0089	-	

2.3 Molecular Dynamics Simulations

For the molecular dynamics simulations, a flexible model of ammonia was employed. Both inter- and intramolecular potentials of ammonia molecules, which are the same as those used in [9-11, 14-16], were taken from [17, 18]. Two molecular dynamics simulations were performed for an average temperature of 240 K and atmospheric pressure. We used the experimental density of liquid ammonia at the simulated temperature and pressure of 0.688 g/cm³ [19], so a cube containing one calcium ion and 215 ammonia molecules has edges of length 20.67 Å. A periodic boundary condition was used, and the shifted force method [20] was employed to make short-range interactions vanish smoothly at the half-box length. The simulations were started from random configurations and were equilibrated for 10,000 time steps. Then they were continued for 80,000 time steps, corresponding to 10 picoseconds, with system configurations collected after every 10 time step. The calculations were performed on the workstations of the Austrian-Thai Center for Computer Assisted Chemical Education and Research and the National Electronic and Computer Technology Center, Bangkok, Thailand.

3. Results and Discussion

3.1 The Two- and Three-body Potential Functions

Figure 1 indicates good agreement between the SCF two-body and fitted energies, using the parameters given in Table 1. The optimal Ca(II)-N distance and the corresponding SCF energy for the most favourable configuration are 2.41 Å and -62.6 kcal·mol⁻¹, respectively.

The quality of the fit to the three-body correction energies is shown in Figure 3, where the SCF and fit energies are compared. Changes $\Delta E_{3b \, \text{fit}}$ with the distance between Ca(II) and the two nitrogen atoms, r_1 and r_2 , and of the angle between them, θ , can be clearly seen from Figure 4. Three-body effects are strong only when the two ammonia molecules are closer than 3 Å from Ca(II), and are negligible when the distance is greater than about 5 Å. All plots in Fig. 4 show two maxima near $r_2 = r_{op}$ and $\theta=0^{\circ}$ or 180° and a saddle point near $r_2=r_{\rm op}$ and θ =90°, where r_{op} denotes the optimal Ca(II)-N distance in the Ca(II)-NH₃ pair potential. In addition, the threebody energy at $\theta = 0^{\circ}$ shows strongest repulsion, and the three-body energy at θ =180° is about two times greater than that at θ =90°. The strongest interaction, for r_2 = r_{op} and $\theta=0^{\circ}$, where the two Ca(II)-N vectors are parallel, cannot occur in the solution. It is interesting to note that among the plots in Fig. 4, the one with r_1 =2.0 Å shows the strongest three-body effects. Note also that the three-body correction energies involve only the ammonia molecules in the first solvation shell of Ca(II). In practice, the strongest repulsive effect will be near r_1 = r_2 = r_{op} and θ =180°. The corresponding value of ΔE_{3b} is about 10 kcal·mol⁻¹. This is about 20% of the most negative interaction in the Ca(II)-NH₃ pair potential at the same distances.

3.2 Structural Properties of the Solution

Ion-solvent Structure

The solvation structure of the solution can be analyzed from the radial distribution functions (RDFs) of pairs of all species involved in the solution. The Ca-N and Ca-H RDFs as well as the corresponding integration numbers obtained for each simulation are calculated and compared in Figs. 5a and 5b, respectively.

Without the three-body correction, the Ca-N RDF shows the first sharp peak centered at 2.53 Å. The integration number up to the first minimum of 3.25 Å is exactly 9. With the three-body correction, the first peak shifts to 2.86 Å, the first minimum is at 3.98 Å and the first shell coordination number reduces to 8. It is interesting to note that the shift of the first peak position by 0.33 Å in this study is much higher than the increase by 0.12 Å for Mg(II) [9] and the decrease by 0.08 Å for Zn(II) [10] in liquid ammonia. The significant increase of the size of the first solvation shell for Ca(II) can be understood in terms of the looser binding of the solvent molecules in the bigger solvation sphere for Ca(II) $(r_{op}=2.41 \text{ Å} \text{ and the corresponding stabilization energy,}$ $\Delta E_{\rm op} = -62.6 \, \text{kcal} \cdot \text{mol}^{-1}$) as compared with Mg(II) $(r_{\rm op}=2.06 \text{ Å}, \Delta E_{\rm op}=-95.7 \text{ kcal} \cdot \text{mol}^{-1})$ and Zn(II) $(r_{\rm op}=1.95 \text{ Å}, \Delta E_{\rm op}=-94.1 \text{ kcal} \cdot \text{mol}^{-1})$ [9, 10]. On the other hand, it was found that the calculated size of the first solvation sphere for singly charged Li(I) and Na(I) in ammonia remains unchanged when the three-body corrections are applied [10, 11].

The influence of the three-body corrections on the second peak of the Ca(II)-N RDF is also different from that on the other doubly charged ions, Mg(II) and Zn(II). As a consequence of the loosely bound solvation sphere of Ca(II), the three-body effect causes the disappearance of a well recognized second peak of the Ca(II)-N, RDF, while this effect for Mg(II) and Zn(II) leads to a slight shift of the second peak to longer distances.

The Ca(II)-H RDFs of simulations with and without three-body corrections show a sharp first peak at 3.39 Å and 3.10 Å containing 27 and 24 hydrogen atoms, respectively. Changes due to the three-body corrections are

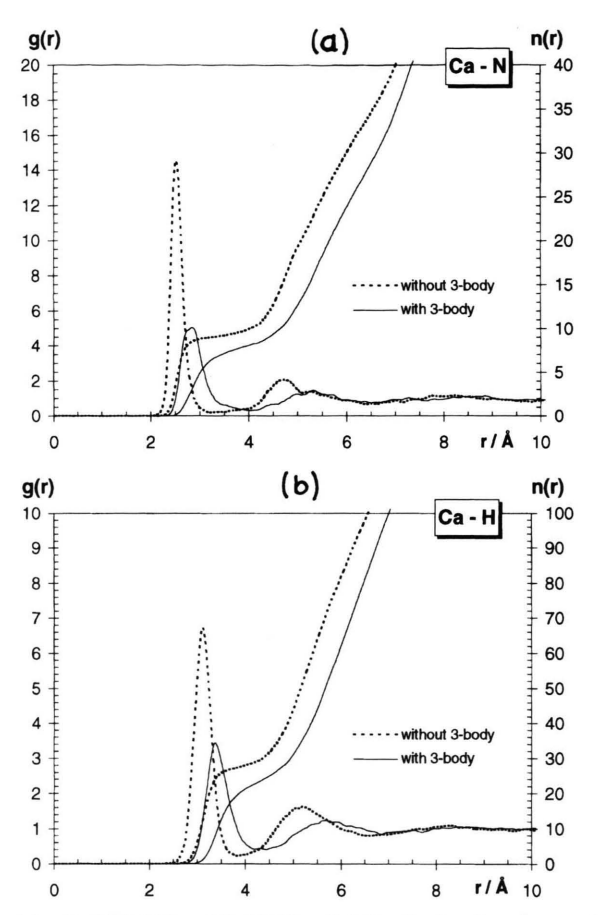


Fig. 5. Ca(II)-N and Ca(II)-H radial distribution functions and corresponding running integration numbers for simulations without and with three-body corrections.

similar to those for the Ca(II)-N RDF. As expected, no significant difference has been detected between the N-N, N-H and H-H RDFs of the two runs. Their characteristics, as well as those of the Ca(II)-N and Ca(II)-H RDFs have been summarized in Table 3.

To monitor the short-range structure of the 9 (8) ammonia molecules in the first solvation shell for simulations without (with) three-body corrections, we examine the configuration-averaged distribution of the N-Ca-N angle for pairs of solvent molecules in the first shell (Figure 6). Note that the optimal spacing of 8 solvent molecules equidistant from the solute would give rise to a cubic configuration. With respect to a given solvent molecule, 3 other molecules would be at an N-Ca(II)-N angle of 70.5°, another 3 at 109.5°, and 1 at 180°; the cosines of these angles are 1/3, -1/3, and -1, respectively. The simulation results without three-body corrections show a sharp peak centered close to 1/3 and a large gap between that peak and a further peak ($\cos \alpha \cong 1/3$), indicating a cubic structure that is distorted to accommodate a ninth molecule. When three-body corrections are included, the distribution is qualitatively similar, but the peaks are much broader, indicating that the expected structure of the 8 ammonia molecules in the first solvation shell is a less rigid, time-varying, distorted cubic configuration.

Figure 7 shows the distribution of $\cos\beta$ which is defined as the angle between the vector pointing from the calcium ion to the nitrogen atom and the dipole vector for an ammonia molecule located in the first solvation shell. The distributions obtained from both simulations are sharply peaked at $\cos\beta=1.0$, with no significant difference between them. The distribution for Ca(II) is broader than that for Mg(II) and narrower relative to that of Na(I) [9]. This can be understood in terms of the strength of the interaction energy, $-\mu E \cos\beta$, between the ammonia dipole moment, μ , and the ion's electric

Table 3. Characteristics of radial distribution functions of Ca(II): R_i , r_{Mi} , and r_{mi} are the distances in Å where for the *i*-th time $g_{\alpha\beta}(r)$ is unity, maximized, and minimized, respectively, and $n_{\alpha\beta}(r_{m1})$ is the running integration number up to r_{m1} .

	αβ	R_1	r_{M1}	$g_{\alpha\beta}(r_{M1})$	R_2	r_{m1}	$g_{\alpha\beta}(r_{m1})$	r_{M2}	$g_{\alpha\beta}(r_{M2})$	$n_{\alpha\beta}(r_{m1})$
without 3-body corrections	N N N H H H Ca N Ca H	2.97 2.94 3.10 2.28 2.79	3.30 3.64 3.69 2.53 3.10	2.0 1.2 1.1 15.1 6.8	4.22 4.44 4.51 2.88 3.47	5.07 5.12 5.21 3.25 3.85	0.8 0.9 0.9 0.2 0.2	6.52 6.53 6.68 4.75 5.25	1.1 1.1 1.0 2.1 1.6	12.6 39.1 41.1 8.97 27.4
with 3-body corrections	N N N H H H Ca N Ca H	2.99 2.97 3.08 2.51 3.08	3.34 3.67 3.81 2.86 3.39	2.1 1.2 1.1 5.1 3.4	4.25 4.49 4.55 3.30 3.81	5.13 5.02 5.37 3.98 4.42	0.7 0.9 0.9 0.3 0.4	6.60 6.69 6.73 5.28 5.68	1.1 1.1 1.0 1.5 1.2	12.8 36.8 44.8 8.19 24.3

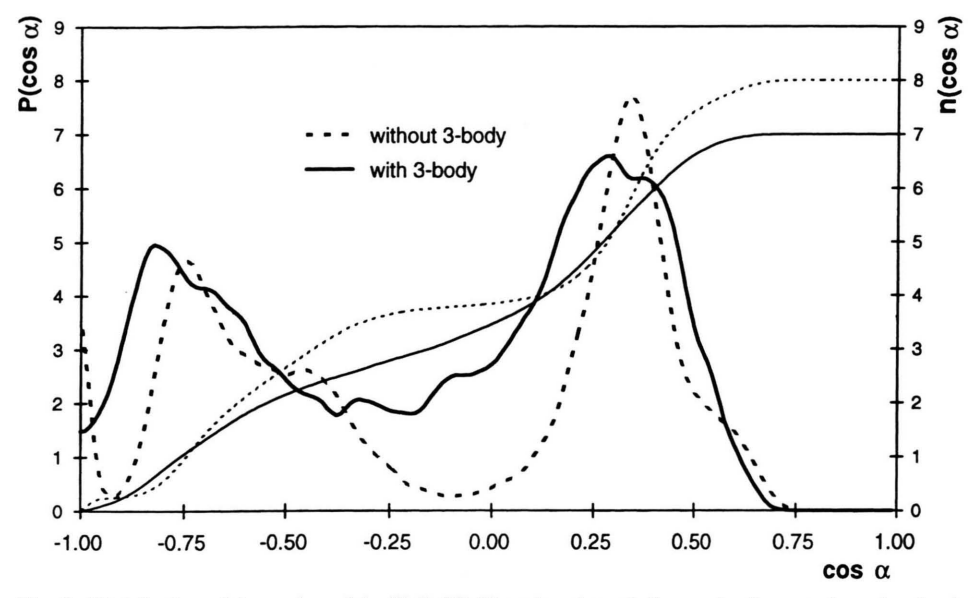


Fig. 6. Distribution of the cosine of the N-Ca(II)-N angle, $p(\cos\alpha)$, for a pair of ammonia molecules in the first solvation sphere and running integration number, $n(\cos\alpha)$.

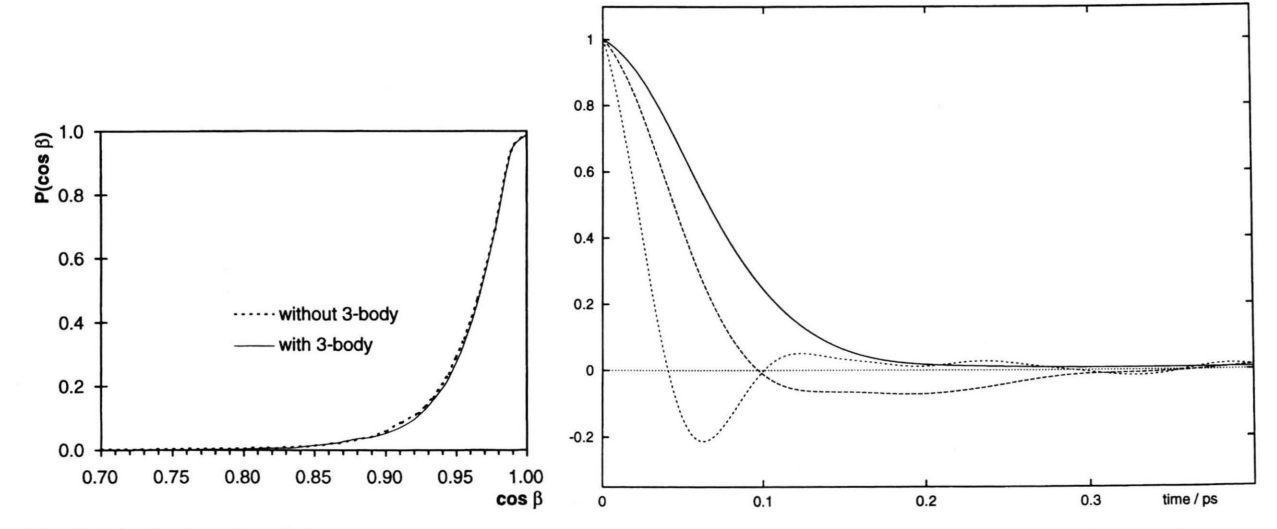


Fig. 7. Distribution of $\cos\beta$ for ammonia molecules in the first solvation shell of calcium ion (see text for details).

Fig. 8. Normalized center of mass velocity autocorrelation functions for ammonia molecules in the bulk (solid line) and the first solvation shell of Ca(II) obtained from our simulations with (long-dashed line) and without (short-dashed line) three-body corrections.

field, $E \propto q/r^2$. Based on our simulations, the strength of the electric field at the first solvation shell is in the order Mg(II)>Ca(II)>Na(I): this explains why Mg(II) has the narrowest $\cos \beta$ distribution and Na(I) has the broadest.

3.3 Dynamical Properties of the Solution

Translational Motions

Translational motions of the molecules can be represented by the velocity autocorrelation function (acf). The center-of-mass acfs of the two simulations, with and

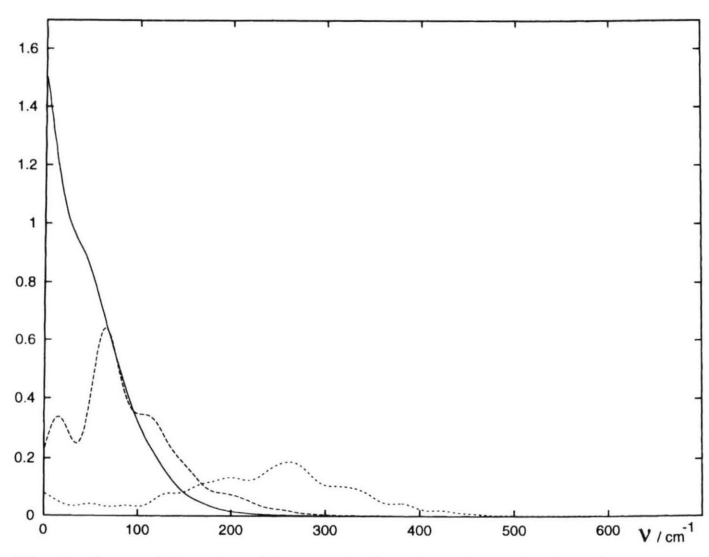


Fig. 9. Spectral density of the translational motions obtained from Fourier transformations of the normalized center of mass velocity autocorrelation functions shown in Figure 8.

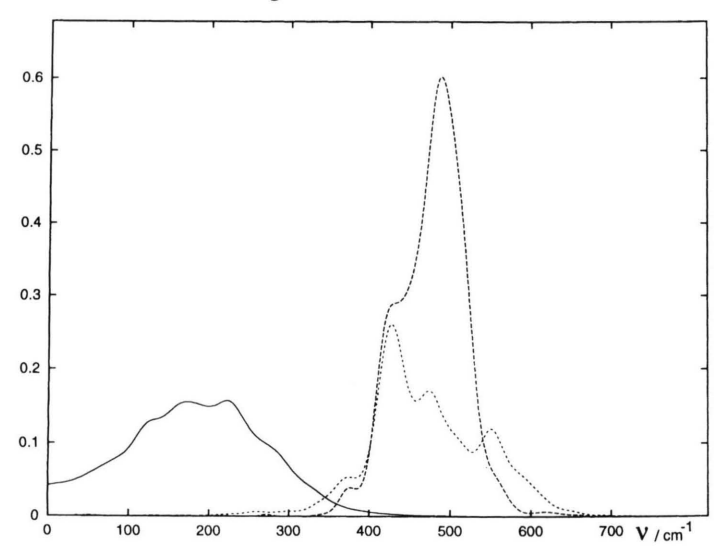


Fig. 10. Spectral density of the rotation about the x axis (defined by the configuration of the first ammonia molecule in Fig. 2) for ammonia molecules in the bulk (solid line) and the first solvation shell of Ca(II) obtained from our simulations with (long-dash line) and without (short-dash line) three hady corrections

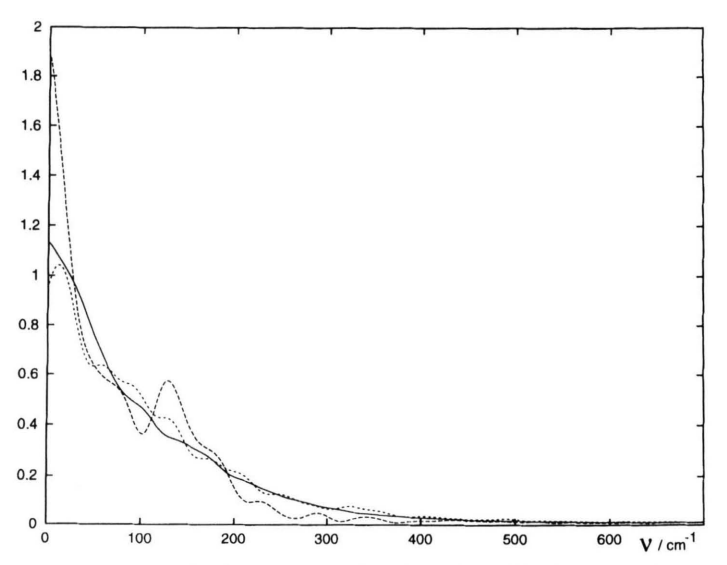


Fig. 11. Spectral density of the rotation about the z (dipole moment) axis for the molecules as defined in Figure 10.

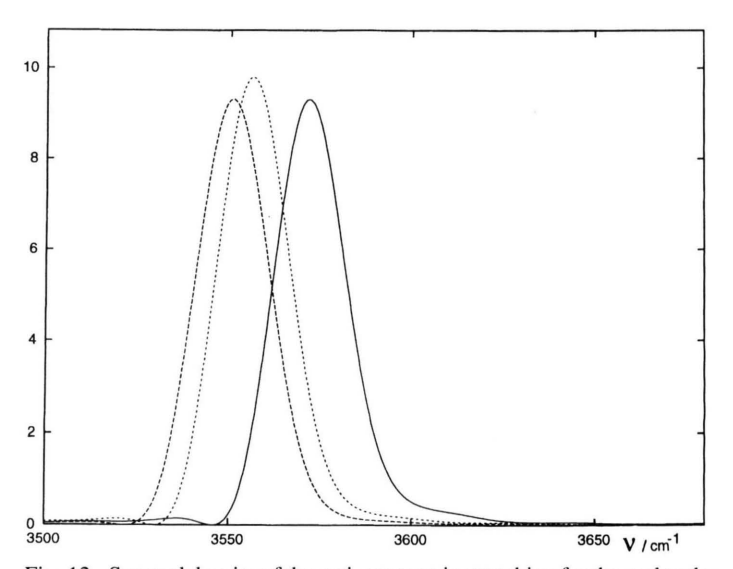


Fig. 12. Spectral density of the anti-symmetric stretching for the molecules as defined in Figure 10.

without the three-body corrections, both for molecules in the bulk and the first solvation shell, have been calculated separately and plotted in Figure 8. Fourier transform, $\Im(\omega)$, is called the spectral density and is defined as

$$\Im(\omega) = \int_{0}^{\infty} C_{\nu}(t) \cos(\omega t) dt, \qquad (4)$$

where $C_{ij}(t)$ denotes the acfs (Figure 9).

The acfs for bulk molecules decay smoothly to zero at about 0.25 ps for both runs. The acf for molecules in the first solvation shell for the simulation, using only the pair potentials, crosses zero at 0.038 ps before overshooting due to a restoring force, which is much faster than the time of 0.086 ps when the three-body effects are included. The spectral densities of the three types of molecules (bulk, first solvation shell with three-body correction and first solvation shell using only pair potentials) peak at 0, 67 and 259 cm⁻¹, respectively (Figure 9). We see that bulk molecules can translate freely (with zero frequency), while solvated molecules are bound more tightly when the three-body corrections are neglected. In conclusion, the acf and spectral density plots confirm that the three-body corrections yield looser binding of the solvated molecules.

It is found experimentally that the self-diffusion coefficient (D) of liquid ammonia is strongly temperature dependent [21], and it is not yet possible to model that properly using simulation data [18, 22]. A self-diffusion coefficient for bulk ammonia calculated in our previous work [18] using the same NH₃-NH₃ pair potential as in this study, and calculated in [22] are approximately 70% too high and 80% too low, respectively, compared with the experimental value at 277 K [21, 23]. However, for the ammonia molecules in the first solvation shell of Ca(II) we obtained $D = (3.80 \pm 2.22) \times 10^{-4} \text{ cm}^2 \text{ s}^{-1}$ and $D=(5.75\pm2.35)\times10^{-5}$ cm² s⁻¹ for the simulations with and without three-body corrections, respectively. The relatively large error is due to the fact that there are only a few ammonia molecules involved in the statistical calculations.

Librational Motions

Librational dynamics of the ammonia molecules in the simulated system can be studied through the Fourier transform of the acf of velocity components of hydrogen atoms. Details of the projections of the velocities onto degenerate axes are explained in [24]. The spectral dia-

Table 4. Comparison of vibrational frequencies (cm⁻¹) from our simulations and experimental results.

Mode	Ca(II)-NH	3 simulations	Pure ammonia experimental data		
	solvation shell	bulk liquid	liquid [25]	gas [17]	
Sym. Bend.	1310	1184	1066	932,968	
Asym. Bend.	1560	1643	1638	1627	
Sym. Stretch.	3251	3418	3240	3336	
Asym. Stretch.	3557	3580	3379	3444	

grams of rotation around x and z axes, defined by the configuration of the first ammonia molecule (N1) in Fig. 2, are shown in Figs. 10 and 11, respectively.

The rotational spectrum around the x axis of the molecules in the bulk peaks near 200 cm⁻¹, while those of solvated molecules for both simulations, with and without three-body corrections are strong between 400 cm⁻¹ to 600 cm⁻¹. The Fourier transforms of the acfs for rotation about the dipole moment axis (Fig. 11) are all quite similar. The maximum at zero frequency indicates fairly free rotation around that axis.

Vibrational Motions

Table 4 shows the consistency between the vibrational frequencies from experiments and from simulations, especially between liquid ammonia and bulk molecules in simulations. From the qualitative agreement in the bulk system, it can be expected that the potentials employed in the simulation lead to a qualitatively correct description of the effect of the calcium ion. The blueshift of the symmetric bending and redshift of the symmetric stretching mode for the molecules in the solvation shell indicates the influence of calcium ion interactions on the ammonia molecules. Similar effects were also found in the system of Li⁺ in liquid ammonia [18] and systems of K⁺ and I in liquid ammonia [14]. The effect of adding threebody corrections on these frequencies was not strong, except for a slightly decreasing shift in the anti-symmetric stretching mode, as shown in Figure 12.

Acknowledgement

Financial support by the Thailand Research Fund and the generous supply of computer time by the Austrian-Thai Center for Computer Assisted Chemical Education and Research in Bangkok and the National Electronic and Computer Technology Center, Bangkok, Thailand are gratefully acknowledged.

- [1] M. J. Elrod and R. J. Saykally, Chem. Rev. **94,** 1975 (1994).
- [2] L. Jansen, Phys. Rev. 125, 1798 (1962).
- [3] E. Lombardi and L. Jansen, Phys. Rev. 167, 822 (1968).
- [4] E. E. Polymeropoulos and J. Brickmann, Chem. Phys. Lett. 92, 59 (1982).
- [5] J. Kim, S. Lee, S. J. Cho, B. J. Mhin, and K. S. Kim, J. Chem. Phys. **102**, 839 (1995).
- [6] T. Lybrand and P. A. Kollman, J. Chem. Phys. 83, 2923 (1985).
- [7] R. Kelterbaum, N. Turki, A. Rahmouni, and E. Kochanski, J. Chem. Phys. 100, 1589 (1944).
- [8] L. X. Dang, J. Chem. Phys. 96, 6970 (1992).
- [9] S. Hannongbua, J. Chem. Phys. 106, 6076 (1997).
- [10] S. Hannongbua, T. Kerdcharoen, and B. M. Rode, J. Chem. Phys. **96**, 6945 (1992).
- [11] S. Hannongbua, Chem. Phys. Lett. (1998) in press.
- [12] W. S. Benedict and E. K. Plyler, Can. J. Phys. 35, 890 (1985).
- [13] R. S. Mulliken, J. Chem. Phys. **23**, 1833, 1841, 2338, 2343 (1955).

- [14] A. Tongraar, S. Hannongbua, and B. M. Rode, Chem. Phys. 219, 279 (1997).
- [15] S. Hannongbua, Aust. J. Chem. 44, 447 (1991).
- [16] S. Hannongbua and B. M. Rode, Chem. Phys. **162**, 257 (1992).
- [17] V. Spirko, J. Mol. Spectrosc. 101, 30 (1983).
- [18] S. Hannongbua, T. Ishida, E. Spohr, and K. Heinzenger, Z. Naturforsch. **43a**, 572 (1988).
- [19] R. C. Weast, Handbook of Chemistry and Physics, 57th ed.; CRC: Ohio 1976–1977.
- [20] W. B. Streett, D. J. Tildeslay, and G. Saville, ACS Symp. Ser. 86, 144 (1978).
- [21] A. N. Garroway and R. M. Cotts, Phys. Rev. A7, 635 (1973).
- [22] R. W. Impey and M. L. Klein, Chem. Phys. Lett. 104, 579 (1984).
- [23] D. E. O'Reilly, E. M. Peterson, and C. E. Scheie, J. Chem. Phys. **58**, 4072 (1973).
- [24] P. Bopp, Chem. Phys. 196, 205 (1986).
- [25] T. Birchall, I. Drummond, J. Chem. Soc. 1970, 1859.